

# Optimization of reaction conditions and effect of catalyst type on product distribution in Cyclooctene oxidation

Yahya Zamani<sup>1,2\*</sup>, Mehdi Bakavoli<sup>2</sup>, Ali Mohajeri<sup>1</sup>, Seyed Mohammad Seyed<sup>2</sup>

<sup>1</sup> Research institute of petroleum industry, Tehran, Iran

<sup>2</sup> Analytical division, Faculty of Chemistry, University of Mazandaran, Babolsar, Iran

---

## Abstract

Oxidation of cyclooctene was studied in presence aqueous hydrogen peroxide (30%, v/v) over nano iron oxide. The catalyst prepared by microemulsion method and characterized using various techniques including XRD, TEM and BET techniques for evaluating phase, structure and morphology and surface area. In this study, we investigated the effects of varying the catalyst content, reaction temperature, H<sub>2</sub>O<sub>2</sub> to cyclooctene molar ratio, reaction temperature and solvent. Epoxycyclooctane was found to be the main reaction product, along with amounts of other products. The best result for epoxycyclooctane production is obtained using acetonitril as solvent at 78 °C for a 16 h reaction period with 0.32 g nano-sized iron particle catalyst. The nano-Fe<sub>2</sub>O<sub>3</sub> catalyst has more conversion and yield than the other iron catalysts in cyclooctene oxidation because of its high surface area and appropriate particle size.

*Keywords:* Nanoparticles iron oxide; Cyclooctene oxidation; Optimization, reaction conditions; Catalyst particle size

© 2016 Published by Journal of Nanoanalysis.

---

## 1. Introduction

The oxidation of organic compounds with an environmentally friendly oxidant, aqueous hydrogen peroxide, is a challenging goal of catalytic chemistry [1-6]. The transformation of hydrocarbons into oxygenated derivatives is an important area of interest for both academic and industrial applications. An active field of research is, thus, the development of efficient catalysts for the oxidation of saturated hydrocarbons in mild conditions [7]. Another interesting line of study is the search for effective, environmentally clean, catalytic reactions to transform cheap natural compounds into valuable intermediates for organic synthesis both in the laboratory and in industry [8]. Among the oxidants available, the use of hydrogen peroxide in the catalytic oxidation of organic compounds has been gaining special attention since it has many advantages when compared to traditional oxidants such as KMnO<sub>4</sub>, Cr<sup>VI</sup> compounds and others [9–11]. Diluted H<sub>2</sub>O<sub>2</sub> is a safe, nontoxic and low-cost reagent, easily manipulated after the reactions.

In general, iron is not the first choice when it comes to the development of novel catalyst systems, but it has a number of advantages over other transition metals (such as Pt, Pd, Rh, Ru or Au) typically utilized as catalysts in organic chemistry. It is cheap, abundant, non-toxic and environmentally friendly. Accordingly, an

---

\* Corresponding Author: E-mail address: teymourim@ripi.ir

increasing number of publications describe the investigation of iron-based catalyst systems in transformations such as carbon-carbon [12] and carbon-heteroatom bond forming reactions [13], oxidations [14-17], reductions [18] and polymerizations [19,20] and other reactions [21]. One of the main products of olefins oxidation are epoxides. Epoxides are important organic intermediates because they undergo ring-opening reactions with a variety of reagents to give mono- or bi-functional organic products [22]. The catalytic epoxidation with hydrogen peroxide as an oxidant might offer some advantages because (i) it generates only water as a by-product and (ii) it has a high content of active oxygen species [23-29]. Nanoparticles of various materials catalyze many important chemical transformations, including oxidation of hydrocarbons, C-C coupling, hydrogenation-dehydrogenation, and redox [30-40].

As compared to their bulk counterparts, nanoparticles often have superior or even new catalytic properties following from their nanometer size that gives them increased surface-to-volume ratios and chemical potentials. So the size of nanoparticles is pivotal in determining their catalytic properties, and understanding how size affects their catalytic properties remains a central goal in nanocatalysis research [4,41-46].

Nanoparticles iron oxide including  $\text{Fe}_2\text{O}_3$  are a class of chemically and thermally stable materials suitable for a wide variety of applications including catalysis. Although the studies on the oxidation catalysts of cycloalkenes are extensive, the investigations on the optimization of reaction conditions are scarce and study of the effect of catalyst particle size on products selectivity has not been investigated. In this paper, we prepared nano iron oxide (hematite) by microemulsion method. The synthesized nanoparticles were characterized by XRD, TEM and BET techniques. The catalytic performance of nano-sized iron oxide has been investigated in the oxidation of cyclooctene with  $\text{H}_2\text{O}_2$  as oxidant to form epoxyoctane and other products in different conditions. Finally we investigated effect of type of iron catalysts in cyclooctene oxidation.

## 2. Experimental

### 2.1. Synthesis of nano- $\text{Fe}_2\text{O}_3$

Nanostructure iron oxides catalyst was prepared by microemulsion method [47]. All the chemicals were analytically pure and used without purifying further. A water solution of metal precursors,  $\text{FeCl}_3 \cdot 6\text{H}_2\text{O}$  was added to a mixture of an oil phase containing 2-Propanol and chloroform with a ratio of 1:1 and sodium dodecyl sulfate (SDS) as a surfactant. Sodium hydroxide in the aqueous phase was added as precipitating agent and stirred for 4 hour. The obtained mixture was left to decant overnight. The solid was recovered by centrifugation and washed thoroughly with distilled water and acetone. Finally, the samples were dried overnight at 120 °C, and subsequently calcined in air at 350 °C for 4 h. Figure1 shows catalyst preparation flow diagram.

### 2.2. Catalyst characterization

BET surface areas were determined by nitrogen physisorption (Micrometrics ASAP 2010). Average particle size of the calcined powders was measured by LEO 912AB TEM. XRD spectra of fresh catalyst was conducted with a Philips PW1840 X-ray diffractometer with monochromatized Cu ( $\text{K}\alpha$ ) radiation for determining of iron phases.

### 2.3. Reaction procedure for the oxidation of cycloocten

Cyclooctene oxidation was carried out in a 50ml two-necked round bottom flask provided with a magnetic bead for stirring and a flask condenser. The first reaction was carried out with varying solvents, which was selected the best solvent for this reaction.

The next study, we were used experimental design method [48], which enables selection of the optimum conditions. A total of 25 sets of experimental data with variation of reaction time and temperature,  $\text{H}_2\text{O}_2$  to cyclooctene molar ratio, and catalyst contents were carried out for this study (Table 1). Experimental conditions were varied in the following ranges:  $t=6-16$  h,  $T = 50-78$  °C,  $\text{H}_2\text{O}_2$  /cyclooctene molar ratio = 0.5-3 and catalyst contents = 0.1-0.5g. GC analyses were performed on Agilent 7890 (FID detector) equipped with column (50 m length\_0.200 mm ID\_0.5  $\mu\text{m}$  film thickness).

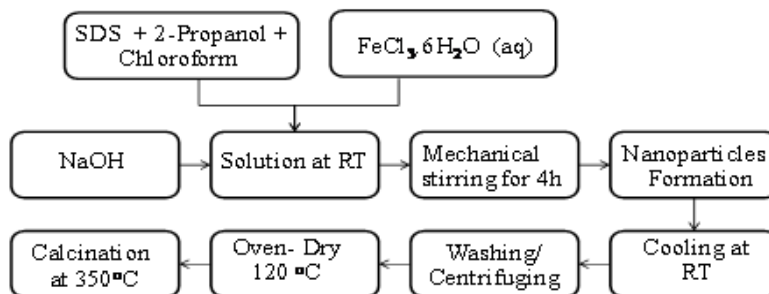


Figure 1. Catalyst preparation flow diagram.

Table 1. Experimental design for catalytic oxidation of cyclooctene with  $H_2O_2$  in different conditions

Exp No.	$H_2O_2$ /Cyclooctene molar ratio	t (h)	T (°C)	Nano iron oxide (gr)
1	0.5	6	65	0.3
2	0.5	16	65	0.3
3	3	6	65	0.3
4	3	16	65	0.3
5	1.7	11	50	0.1
6	1.7	11	50	0.5
7	1.7	11	78	0.1
8	1.7	11	78	0.5
9	0.5	11	65	0.1
10	0.5	11	65	0.5
11	3	11	65	0.1
12	3	11	65	0.5
13	1.7	6	50	0.3
14	1.7	6	78	0.3
15	1.7	16	50	0.3
16	1.7	16	78	0.3
17	0.5	11	50	0.3
18	0.5	11	78	0.3
19	3	11	50	0.3
20	3	11	78	0.3
21	1.7	6	65	0.1
22	1.7	6	65	0.5
23	1.7	16	65	0.1
24	1.7	16	65	0.5
25	1.7	11	65	0.3
26	1.7	11	65	0.3
27	1.7	11	65	0.3

### 3. Results and discussions

The prepared catalyst was characterized for evaluating its morphology and structure.

#### 3.1. Powder X-ray diffraction

X-ray diffraction studies indicate that the materials synthesized are spinels with the cubic phase and all the crystal structures agree with the corresponding reported JCPDS data. The phase composition of the fresh catalysts is determined by XRD analyses as shown Figure2. A definite line broadening of the diffraction peaks is an indication that the synthesized materials are in the nanometer range.

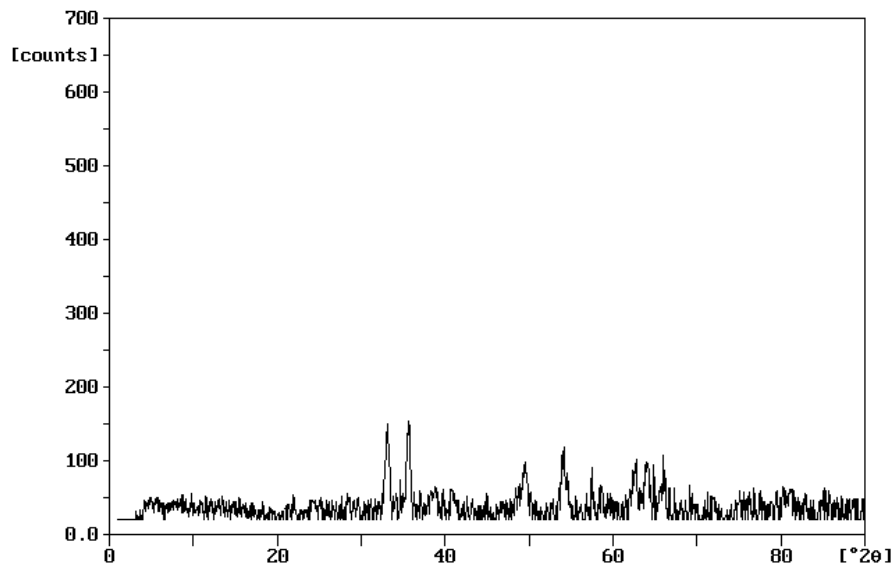
Figure 2. XRD pattern of the nano Fe<sub>2</sub>O<sub>3</sub> catalyst

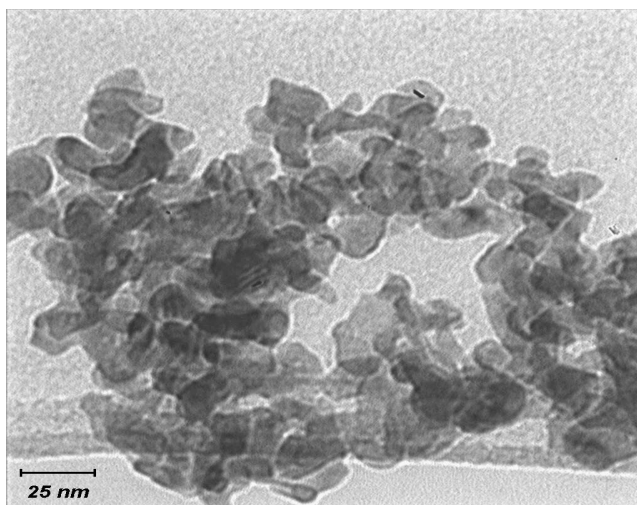
Table 2. Textural properties of the catalyst

Catalyst	BET surface Area (m <sup>2</sup> /g)	Pore Volume (cm <sup>3</sup> /g)	Particle Size dTEM (nm)	Particle Size dXRD (nm)
Nano- Fe <sub>2</sub> O <sub>3</sub>	52.2	0.28	23.9	24.1

### 3.2. Micromeritics ASAP 3020

Surface area, pore volume, and particle size of the catalyst was determined by N<sub>2</sub> physisorption using a Micromeritics ASAP 3020 automated system. A 0.5 g catalyst sample was degassed in the Micromeritics ASAP 3020 at 100 °C for 1 h and then at 300 °C for 2 h prior to analysis. The analysis was done using N<sub>2</sub> adsorption at -196 °C. Table.2 shows the results of ASAP system. The average grain size (crystal diameter) can also be obtained by the Scherrer equation from broadening of the peaks in a wide angle X-ray scattering (WAXS) measurement of the material [49] :

$$d = \frac{kl}{\beta(\theta) \cos\theta}$$

Figure 3. TEM micrograph of the nano Fe<sub>2</sub>O<sub>3</sub> catalyst.

where  $\lambda$  is the X-ray wavelength (nm),  $\beta(\theta)$  the full width at half maximum (rad) of the identification peak,  $\theta$  is the diffraction angle and  $K$  is the typical constant of the equipment.

### 3.3. Transmission electron microscopy

The morphology of Fe<sub>2</sub>O<sub>3</sub> nanoparticles was illustrated by TEM images as shown in Figure 3. The average particle size calculated from the TEM micrographs is consistent with the crystallite size obtained from XRD measurement and is included in Table 2. Although TEM revealed that the nanoparticles diameter was in the range of 20–30 nm.

### 3.4. Optimization of reaction conditions

#### 3.4.1. Influence of the solvents

The influence of solvents were studied by carrying the reaction in different solvents like water (H<sub>2</sub>O), methanol (CH<sub>3</sub>OH), ethanol (C<sub>2</sub>H<sub>5</sub>OH); 1-butanol(C<sub>4</sub>H<sub>9</sub>OH), 2-butanone(C<sub>4</sub>H<sub>8</sub>O); acetone(CH<sub>3</sub>COCH<sub>3</sub>), acetonitrile (CH<sub>3</sub>CN), toluene(C<sub>6</sub>H<sub>5</sub>CH<sub>3</sub>) and n-hexan(C<sub>6</sub>H<sub>12</sub>) on the cyclooctene conversion and selectivity of products over nano-sized iron oxide catalyst. The same reaction was also carried out in absence of solvent in which very less amount of cyclooctene conversion is observed. Since H<sub>2</sub>O<sub>2</sub> (30%) is added these solvents. The selectivity of epoxy cyclooctane and conversion are in the order of C<sub>6</sub>H<sub>12</sub>< C<sub>6</sub>H<sub>5</sub>CH<sub>3</sub><H<sub>2</sub>O<CH<sub>3</sub>OH<C<sub>2</sub>H<sub>5</sub>OH< C<sub>4</sub>H<sub>9</sub>OH < C<sub>4</sub>H<sub>8</sub>O< CH<sub>3</sub>COCH<sub>3</sub>< CH<sub>3</sub>CN. The present study shows high selectivity and high conversion in acetonitrile than the other solvents. The cyclooctene conversion and epoxy cyclooctane selectivity in different solvents were shown in figure 4. Acetonitril is found to be the good solvent, because of its aprotic and dissolving nature for an oxidant without complication due to its amount of solvent polarity (Table 3).

**Table 3.** Solvent characterizations

Exp No.	Solvent	bp, °C	Dipole Moment	Dielectric constant (20°C)
1	Water	100	1.85	80
2	Methanol	68	1.70	33
3	Ethanol	78	1.69	24.3
4	1-Butanol	118	1.66	17.8
5	Acetone	56	2.88	20.7
6	Acetonitril	68-70	3.93	36.6
7	n-Hexan	110.6	0.08	2.02
8	2-Butanon	80	2.78	18.5

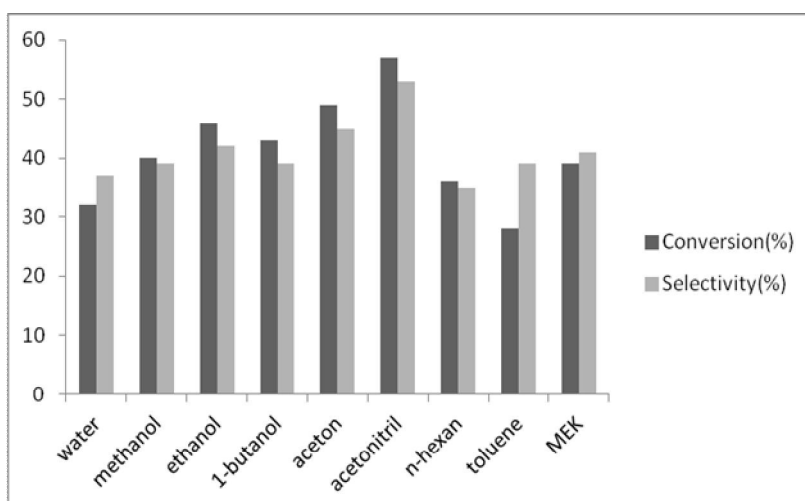


**Figure 4.** Effect of different solvents on cyclooctene oxidation over nano-Fe<sub>2</sub>O<sub>3</sub>. Reaction conditions: H<sub>2</sub>O<sub>2</sub>: Cyclooctene molar ratio 3; reaction temperature 75 °C; Nano Fe<sub>2</sub>O<sub>3</sub> 0.3 g; 16 h reaction.



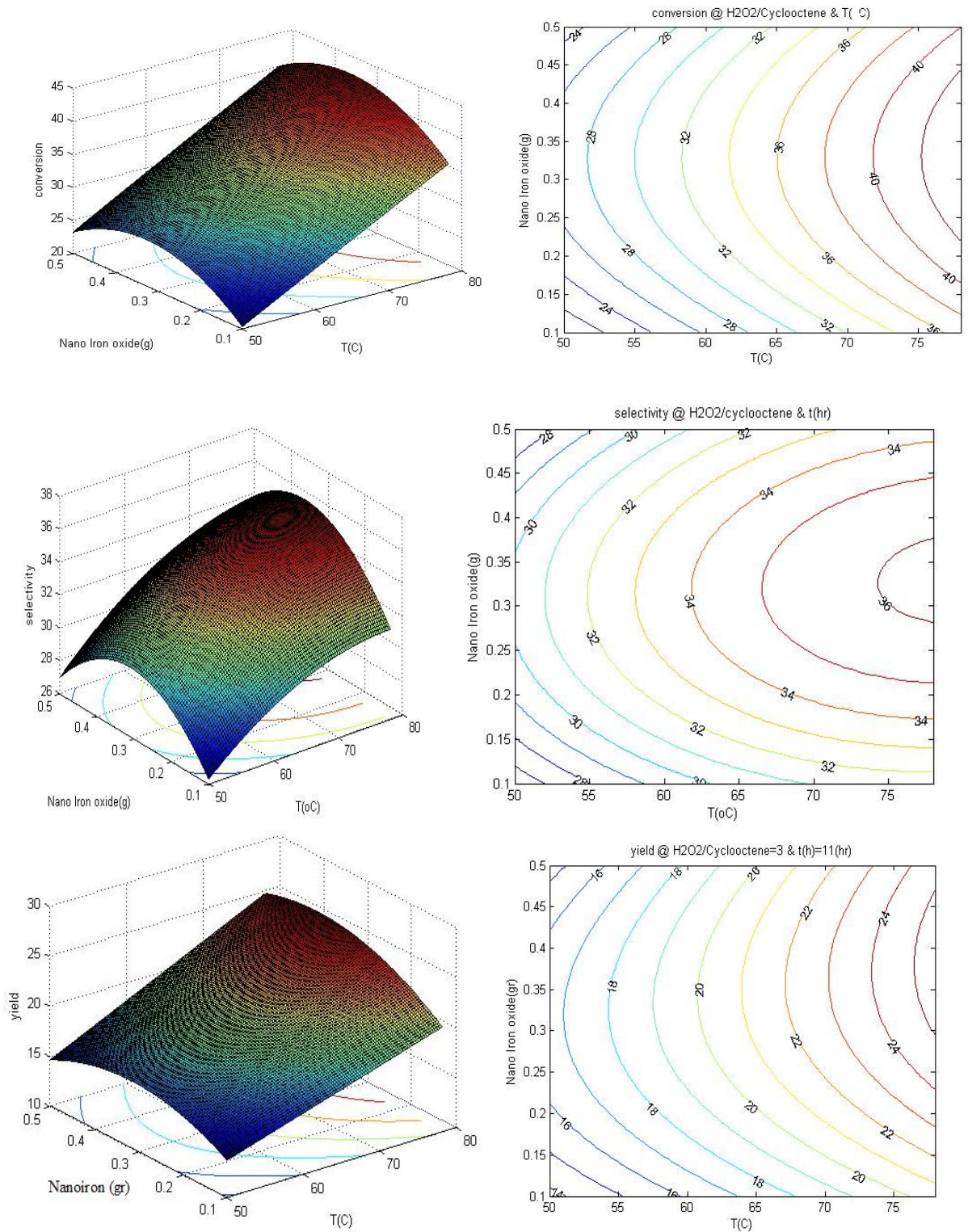


**Figure 5.** The effect of nanoiron content and reaction temperature on the conversion, epoxy cyclooctane selectivity and yield.

The selectivity of epoxy cyclooctane is a maximum (53.2%) in acetonitril with 57.1% conversion. This effect of solvents strongly supports that the selective oxidation of cyclooctene to epoxy cyclooctane takes place through radical mechanism. Solvent effect confirms a free radical mechanism is involved in cyclooctene oxidation over a heterogeneous catalyst.

The nano-Fe<sub>2</sub>O<sub>3</sub> (hematite) are known to be highly efficient epoxidation catalyst which have been successfully used to heterogeneously catalyze the transfer of an oxygen atom from oxidizing agent into hydrocarbon molecules in different solvents. Aprotic solvents like acetone, acetonitrile, etc. are more favorable than protic solvents for the formation of epoxy cyclooctane. The oxidation of cyclooctene to epoxy cyclooctane and other products was used as a model reaction.

#### 3.4.2. Influence of nanoiron content and reaction temperature

The effect of reaction temperature and catalyst amount on the conversion, epoxy cyclooctane selectivity and yield are shown in figure.5. From these figures, it can be found that the reaction conversion, epoxy cyclooctane selectivity and yield increased with increasing temperature. Increasing the catalyst amount from 0.10 to 0.32 gr increased the conversion, epoxy cyclooctane selectivity and yield and increasing catalyst amount higher than 0.32 gr decreased cyclooctene conversion, epoxy cyclooctane selectivity and yield.

A free radical mechanism may be involved in oxidation of cyclooctene over nano-Fe<sub>2</sub>O<sub>3</sub> catalyst. In case of cyclooctene oxidation in presence of H<sub>2</sub>O<sub>2</sub> (30%) as oxidant, free radicals can be generated on the surface of catalyst, where catalyst accelerates the decomposition of hydrogen peroxide into free radicals. In order to check the role of nano iron oxide towards selective oxidation of cyclooctene, a blank reaction was carried out using 30% H<sub>2</sub>O<sub>2</sub>, Acetonitril (10 ml) and temperature 78 °C, and the reaction was stirred under the similar reaction conditions for 6 h. In absence of nano-Fe<sub>2</sub>O<sub>3</sub> catalyst no reaction takes place as seen from GC analysis.

#### 3.4.4. Influence of cyclooctene /H<sub>2</sub>O<sub>2</sub> molar ratio and reaction time

The effect of cyclooctene /H<sub>2</sub>O<sub>2</sub> molar ratio and reaction time on the conversion, epoxy cyclooctane selectivity and yield are shown in figure 6. As seen, increasing H<sub>2</sub>O<sub>2</sub> concentration and reaction time, the conversion, epoxy cyclooctane selectivity and yield increased. This increase can be explained that increasing H<sub>2</sub>O<sub>2</sub> concentration leads to increase radical oxygen concentration and consequently to increase the reaction the conversion, epoxy cyclooctane selectivity and yield with the increase of reaction time. The interaction of two factors of H<sub>2</sub>O<sub>2</sub> to cyclooctene ratio and reaction time results in a positive effect and increased the reaction conversion, selectivity and yield. Under these reaction conditions, the reaction was carried out by varying the time from 6 h to 16h. As the reaction time increases from 6 to 16 h, cyclooctene conversion increased from 30 to 60 % with 48% selectivity of epoxy cyclooctane. At 16 h yield of epoxy cyclooctane increases up to is 24%, along with the formation of by products like 1-cycloocten-3-ol and 2-cyclooctenone. The result indicates that as the reaction is run for long time the selectivity of byproducts decreased. The results for cyclooctene conversion and selectivity were determined with the accuracy of ±3% error.

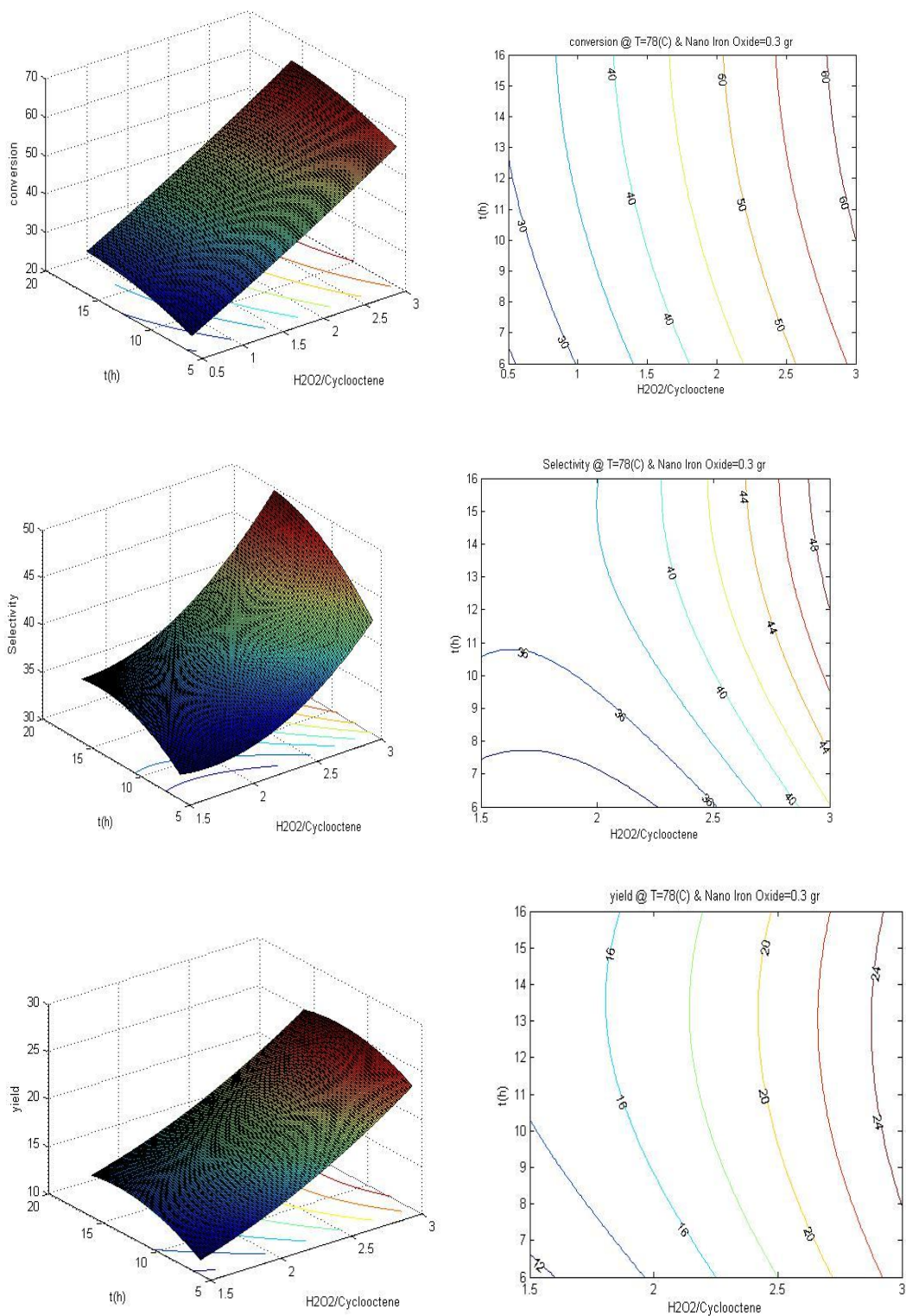


**Figure 6.** The effect of H<sub>2</sub>O<sub>2</sub>/Cyclooctene molar ratio and reaction time on the conversion, epoxy cyclooctane selectivity and yield.



### 3.4.5. Influence of H<sub>2</sub>O<sub>2</sub>/cyclooctene molar ratio and reaction temperature

Figure 7 shows the changes of the conversion, epoxy cyclooctane selectivity and yield with H<sub>2</sub>O<sub>2</sub>/Cyclooctene ratio and temperature. The response of the reaction towards raise in temperature has been studied at different temperatures from 50 °C to 78°C. The reaction was carried out by using H<sub>2</sub>O<sub>2</sub> to cyclooctene molar ratio from 0.5 to 3, over 0.1 – 0.5 g of Fe<sub>2</sub>O<sub>3</sub> catalyst in 10 ml of acetonitril as solvent for 6 - 16 h. As H<sub>2</sub>O<sub>2</sub> to cyclooctene molar ratio increases to 3, the cyclooctene conversion increases from 30 to 50%, further increase in temperature is favorable for the cyclooctene oxidation. When the same reaction was carried out at 78 °C, the epoxy cyclooctane selectivity sharply increases to 44 %. Further rise in temperature (78 °C) the marginal increment in yield was observed (24%). These results indicate that the epoxidation of C=C bond is favorable with increase in temperature up to 78 °C. The results for cyclooctene conversion and selectivity of all the products were determined with the accuracy of ±3% error. However, it can be observed that with the increase of the H<sub>2</sub>O<sub>2</sub> ratio and the reaction temperature, the conversion, epoxy cyclooctane selectivity and yield increased.

With the increase in reaction temperature, conversion as well as the selectivity for epoxy cyclooctane increases. This confirms that at higher temperatures to 78 °C, C=C bond epoxidation is more favorable. It is seen that the cyclooctene conversion increases with the increase in reaction time and selectivity for epoxy cyclooctane increases too, and the formation of other products (1-Cycloocten-3-ol and 2-Cyclooctenone) decreases. As results mentioned above, increasing in all parameters (T, t, H<sub>2</sub>O<sub>2</sub>:Cyclooctene molar ratio) leads to increase in epoxy cyclooctane selectivity except for catalyst amount which just up to extent up to 0.32g caused to increase in the selectivity. However, the conversion as well as the selectivity is found to be best when the hydrogen peroxide:cycloocten molar ratio equal to 3 and the reaction time is 16 h. The optimum conditions based experimental design obtained for the reaction in table 4. So we can conclude that the optimum conditions are acetonitril as solvent at 78 °C for a 16 h reaction period with 0.32 g nano-Fe<sub>2</sub>O<sub>3</sub> catalyst.

**Table 4.** The optimum conditions for cyclooctene oxidation

Reaction Performance	H <sub>2</sub> O <sub>2</sub> /Cyclooctene Molar ratio	t (h)	T (°C)	Nano iron oxide(gr)	Maximum (%)
Conversion (%)	3	16	78	0.32	62.93
Selectivity (%)	3	16	78	0.35	70.65
Yield (%)	3	11.9	78	0.37	43.16

### 3.4.6. The effect of catalysts type

Oxidation of cyclooctene with different catalysts were studied too. Figure 8 shows the effect of type and particle size of iron based catalysts on the conversion, epoxy cyclooctane selectivity and yield over cyclooctene oxidation.

The results presented in Figure 8 shows that nano-Fe<sub>2</sub>O<sub>3</sub> is higher conversion and yield than the other iron catalysts for cyclooctene oxidation due to a high surface area and appropriate particle size.

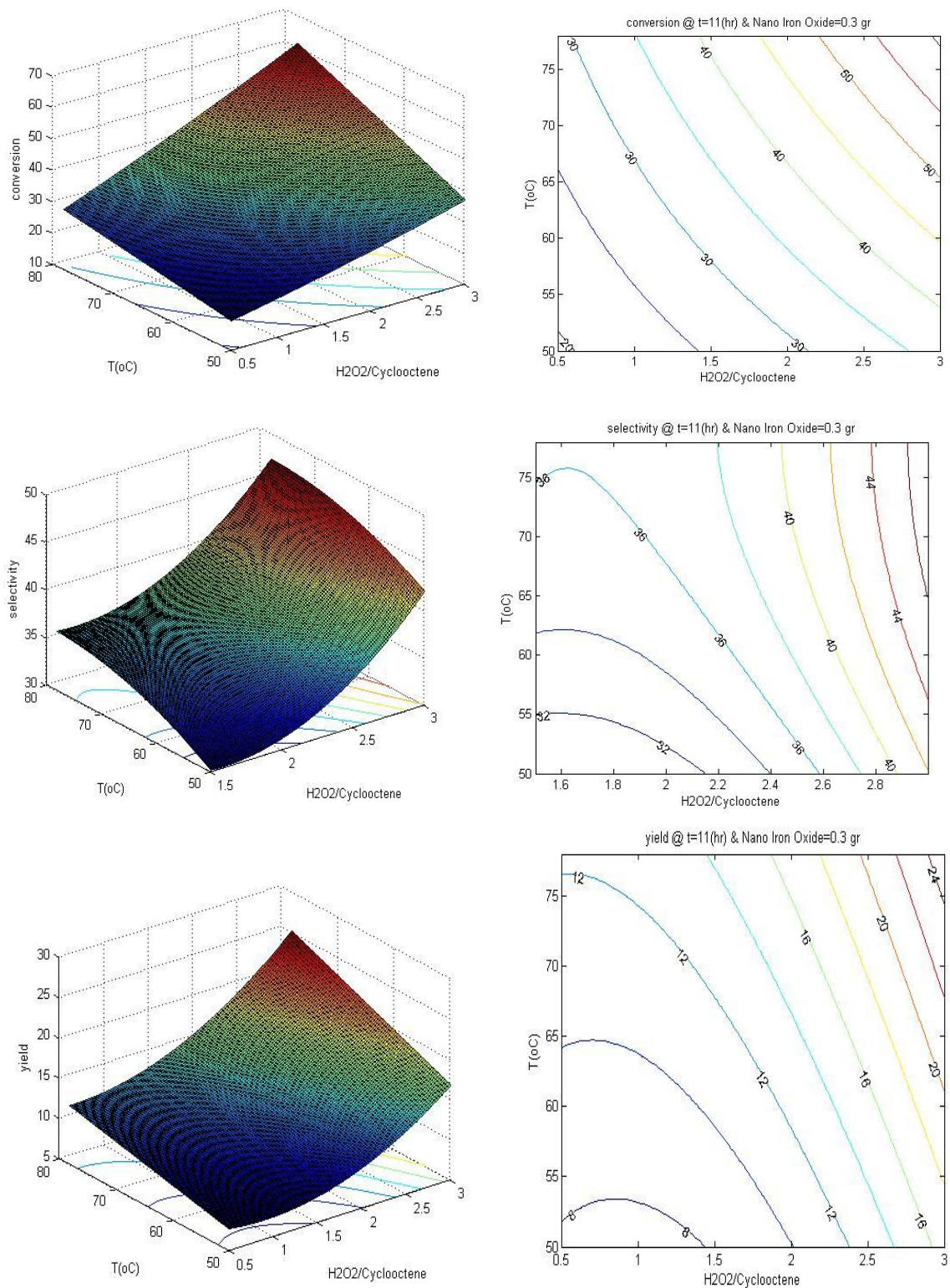


**Figure 7.** The changes of the conversion, epoxy cyclooctan selectivity and yield with H<sub>2</sub>O<sub>2</sub>/Cyclooctene ratio and reaction temperature.

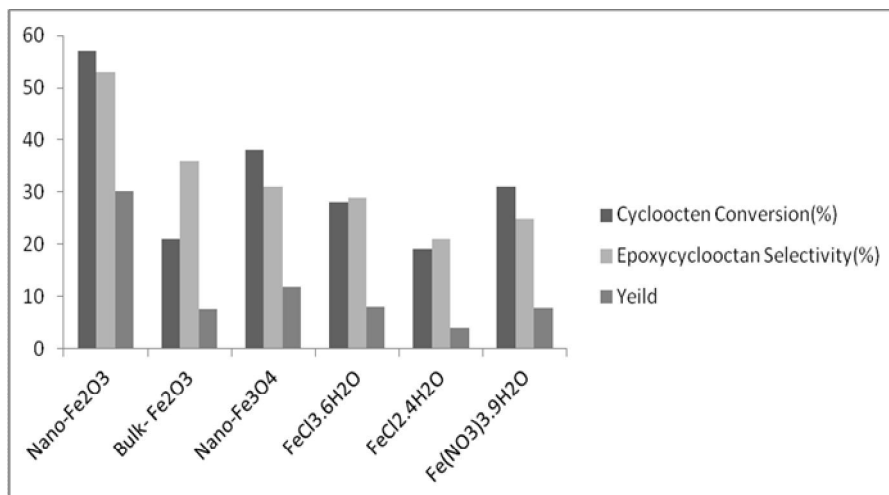
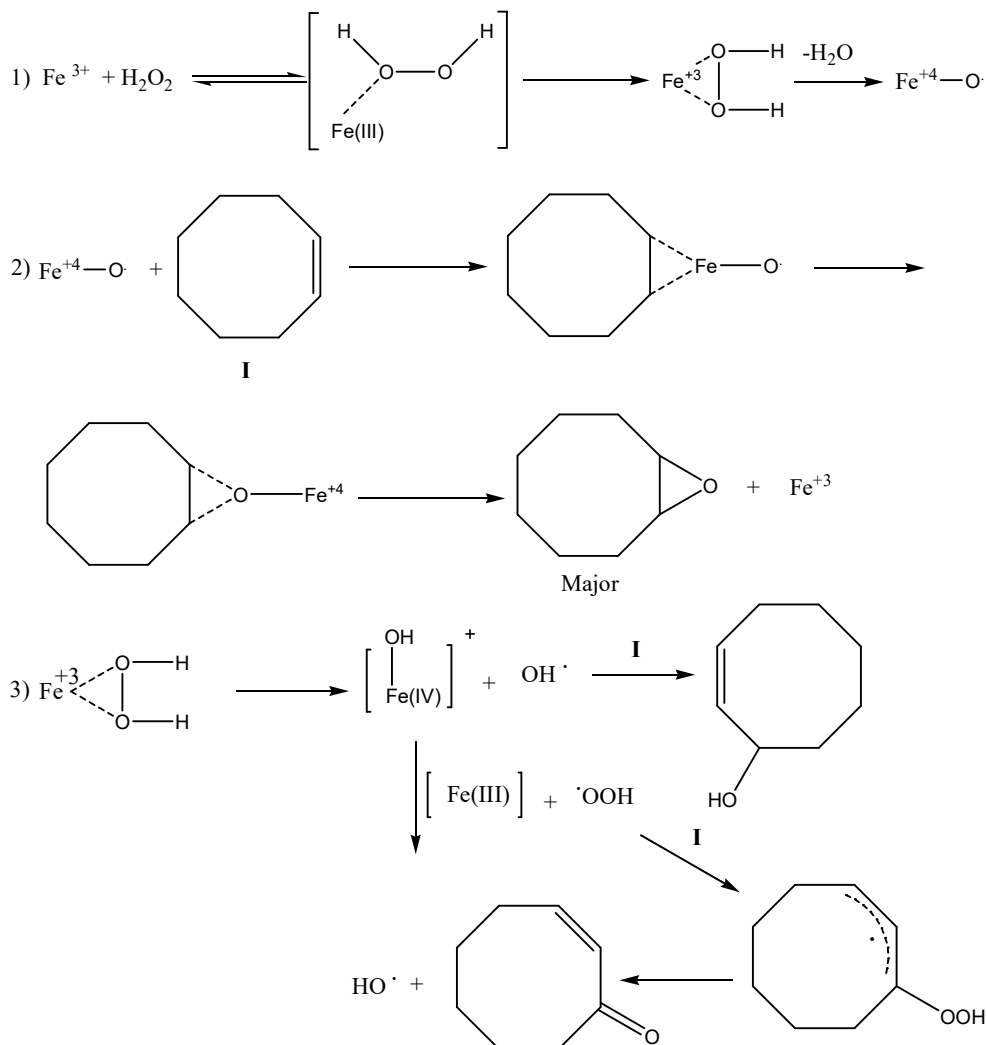


**Figure 8.** The effect of catalyst particle size on the conversion, epoxy cyclooctan selectivity and yield  
 Reaction Conditions: H<sub>2</sub>O<sub>2</sub>: Cyclooctene molar ratio 3; reaction temperature 78 °C; Solvent CH<sub>3</sub>CN (10 cc); 16 h reaction



### 3.5 Investigation of mechanism of the cyclooctene oxidation reaction

The hydrogen peroxide decomposition promoted by transition metal oxide take place by radical reactions. Catalytic activation of H<sub>2</sub>O<sub>2</sub> is achieved, e.g. by the mechanism summarized in scheme 1. In Scheme 1, the formation of metal-oxy radical (Fe<sup>4+</sup>-O<sup>•</sup>) on the catalyst surface is the initiation step of the reaction and the propagation of the reaction chain occurs in solution. A highest yield of cyclooctene is possibly due to further oxidation of cyclooctene oxide formed in the first step by a nucleophilic attack of Fe<sup>4+</sup>-O<sup>•</sup> on the intermediate carbon-carbon double bond. This may be due to significantly amount of H<sub>2</sub>O<sub>2</sub>. H<sub>2</sub>O<sub>2</sub> could freely coordinate to metal and decompose to form metal-oxy radical.

### 4. Conclusion

Nanosized iron oxide catalyst was prepared by the microemulsion method. The type catalyst are found to be highly active for the oxidation of cycloocten with H<sub>2</sub>O<sub>2</sub> oxidant due to their high dispersity, and large surface area, i.e. providing more active sites for the catalytic reaction. Cycloocten undergo a C=C bond oxidation preferentially over the catalyst to give epoxycyclooctan. 2-cyclooctenone and 1-Cycloocten-3-ol are by-products in optimum condition. Thus, we can conclude that most favorable conditions for the oxidation of cyclooctene to epoxycyclooctane is obtained with Fe<sub>2</sub>O<sub>3</sub> as a catalyst, acetonitril as the reaction medium and reaction temperature maintained at 78 °C for 16 h. The effect of type and particle size of iron based catalysts on the catalytic activity and product selectivity has been observed.

### 5. Acknowledgements

We thank the Research and Development of National Iranian Oil Company (NIOC) for financial support and we dedicated this work to the deceased professor Mohammad Rahimizadeh.

### References

- [1] C.T. Kresge, M.E. Leonowicz, W.J. Roth, J.C. Vartuli, J.S. Beck, *Nature* 359 (1992) 710.
- [2] V. Meynen, P. Cool, E.V. Vansant, *Microp. Mesop. Mater.* 129 (2009) 170.
- [3] A. Corma, *Chem. Rev.* 97 (1997) 2373.
- [4] A. Taguchi, F. Schuth, *Microp. Mesop. Mater.* 77 (2005) 1.
- [5] Y. Xu, Z. Wu, L. Zhang, H. Lu, P. Yang, P.A. Webley, D. Zhao, *Anal. Chem.* 81 (2009) 503.
- [6] T. Kamegawa, D. Yamahana, H. Yamashita, *J. Phys. Chem. C* 114 (2010) 15049.
- [7] K. Nakanishi, N. Tanaka, *Acc. Chem. Res.* 40(2007) 863.
- [8] I.I. Slowing, J.L. Vivero-Escoto, C.W. Wu, V.S.Y. Lin, *Adv. Drug Deliv. Rev.* 60 (2008) 1278.
- [9] N.K. Mal, M. Fujiwara, Y. Tanaka, *Nature* 421 (2003) 350-353.
- [10] M.A. Zanjanchi, A. Ebrahimian, Z. Alimohammadi, *Optical Mater.* 29 (2007) 794.
- [11] Y. Wang, F. Caruso, *Chem. Mater.* 17 (2005) 953.
- [12] C. Lei, Y. Shin, J. Liu, E.J. Ackerman, *Nano Lett.* 7 (2007) 1050.
- [13] Y.L. Zhao, Z. Li, K. Kabehie, Y.Y. Botros, J.F. Stoddart, J.I. Zink, *J. Am. Chem. Soc.* 132 (2010) 13016.
- [14] M.T. Janicke, C.C. Landry, S.C. Christiansen, S. Birtalan, G.D. Stucky, B.F. Chmelka, *Chem. Mater.* 11 (1999) 1342.
- [15] M.T. Janicke, C.C. Landry, S.C. Christiansen, D. Kumar, G.D. Stucky, B.F. Chmelka, *J. Am. Chem. Soc.* 120 (1998) 6940.
- [16] R.M. Grudzien, B.E. Grabicka, M. Jaroniec, *J. Mater. Chem.* 16 (2006) 819.
- [17] K.W. Gallis, C.C. Landry, *Adv. Mater.* 13 (2001) 23.
- [18] J.E. Martin, M.T. Anderson, J. Odinek, P. Newcomer, *Langmuir* 13 (1997) 4133.
- [19] D. Zhao, P. Yang, D.I. Margolese, B.F. Chmelka, G.D. Stucky, *Chem. Commun.* (1998) 2499.
- [20] N. Yao, A.Y. Ku, N. Nakagawa, T. Lee, D.A. Saville, I.A. Aksay, *Chem. Mater.* 12 (2000) 1536.
- [21] B. Tian, X. Liu, C. Yu, F. Gao, Q. Luo, S. Xie, B. Tu, D. Zhao, *Chem. Commun.* (2002) 1186.
- [22] A. Hozumi, Y. Yokogawa, T. Kameyama, K. Hiraku, H. Sugimura, O. Takai, M. Okido, *Adv. Mater.* 12 (2000) 985.
- [23] S. Kawi, M.W. Lai, *Supercritical fluid extraction of surfactant from Si-MCM-41. AIChE J.* 48 (2002) 1572.
- [24] Z. Huang, L. Huang, S.C. Shen, C.C. Poh, K.S. Hidajat, N.S.C. Kawi, *Microp. Mesop. Mater.* 80 (2005) 157.
- [25] M. Kruk, M. Jaroniec, C.H. Ko, R. Ryoo, *Chem. Mater.* 12 (2000) 1961.

- [26] S. Inagaki, Y. Sakamoto, Y. Fukushima, O. Terasaki, *Chem. Mater.* 8 (1996) 2089.
- [27] D.Y. Zhao, Q.S. Huo, J.L. Feng, B.F. Chmelka, G.D. Stucky, *J. Am. Chem. Soc.* 120 (1998) 6024.
- [28] M. Kruk, M. Jaroniec, Y. Sakamoto, O. Terasaki, R. Ryoo, C.H. Ko, *J. Phys. Chem. B* 104 (2000) 292.
- [29] A. Galarneau, D. Desplandier, R. Dutartre, F. Di-Renzo, *Microp. Mesop. Mater.* 27 (1999) 297.
- [30] C.G. Sonwane, S.K. Bhatia *J. Phys. Chem. B* 104 (2000) 9099).